Automatic Seizure Detection Using Logarithmic Euclidean-Gaussian Mixture Models (LE-GMMs) and Improved Deep Forest Learning

Shasha Yuan, Xiang Liu, Junliang Shang, *Member, IEEE*, Jin-Xing Liu, *Member, IEEE*, Juan Wang, *Member, IEEE*, and Weidong Zhou

***Abstract*—Automatic seizure detection could facilitate early detection, improve treatment planning, and reduce medical workload. This study describes a novel Logarithmic Euclidean-Gaussian Mixture Models (LE-GMMs) and an improved Deep Forest learning algorithm for epileptic seizure detection. The LE-GMMs could map the Riemannian manifold structure of Gaussian models to linear Euclidean space, which fully exploits the ability of GMMs to distinguish non-seizure and seizure EEG signals. The Multi-Pooling and error Screening Forest (MPSForest) learning method based on Deep Forest uses multi-pooling and out-of-bagging (OOB) error screening to reduce memory load and random tree construction. Firstly, variational modal decomposition (VMD) is applied to decompose electroencephalogram (EEG) signals into five layers, and the first three layers are chosen to construct EEG time-frequency distribution. Then Gaussian Mixture Models are estimated, and the LE-GMMs are constructed to extract valid EEG features. These features are input into the MPSForest model to classify seizure and non-seizure samples. After that, the outputs are subjected to post-processing to get the final seizure detection results, including moving average filtering and the adaptive collar technique. The proposed method achieves average sensitivity of 98.22% and specificity of 98.99% on the UPenn and Mayo Clinic dataset, and for the long-term Freiburg EEG dataset with 21 patients, the sensitivity of 98.47% and specificity of 98.57% are yielded respectively with the false detection rate of 0.24/h. The experimental results show that this proposed method has excellent accuracy in distinguishing non-seizure and seizure EEG signals and holds great potential for clinical research and diagnostics.**

***Index Terms*—Electroencephalogram, seizure detection, logarithmic euclidean-Gaussian mixture models, multi-pooling and error screening forest.**

Manuscript received 21 July 2022; revised 22 November 2022; accepted 12 December 2022. Date of publication 20 December 2022; date of current version 7 March 2023. This work was supported by the National Natural Science Foundation of China under Grants 61902215, 62172254, and 62172253. *(Corresponding author: Shasha Yuan.)*

Shasha Yuan, Xiang Liu, Junliang Shang, Jin-Xing Liu, and Juan Wang are with the School of Computer Science, Qufu Normal University, Rizhao 276826, China (e-mail: jiayouyss@126.com; liuxiang12456@163.com; shangjunliang110@163.com; sdcavell@126.com; wangjuansdu@163.com).

Weidong Zhou is with the School of Microelectronics, Shandong University, Jinan 250100, China (e-mail: wdzhou@sdu.edu.cn).

Digital Object Identifier 10.1109/JBHI.2022.3230793

I. Introduction

Epilepsy is a chronic disease characterized by sporadic episodes of uncontrolled neuronal hyperexcitation (seizure activity) that may spread from a point of origin (focus) to surrounding brain tissue, resulting in various motor, sensory, cognitive, and psychological manifestations [1]. Moreover, severe seizures may endanger human life, and recurrent seizure activity can induce lasting changes in brain structure and function, so early diagnosis and effective control are critical for long-term health. The electroencephalogram (EEG) is an important tool for epilepsy diagnosis and can reveal much information about disease pathology, including focus and pattern of spread [2]. In clinical practice, seizures are detected and assessed by visual observation of EEG changes, which is both time-consuming and burdensome. As an alternative, computer-assisted detection and therapy can facilitate early diagnosis and characterization for timely and effective patient management.

Many automatic epilepsy detection algorithms have been proposed that recognize the temporal, spectral, and spectral-temporal characteristics of epileptic form EEG [3], [4]. For instance, Ru et al. used variational modal decomposition (VMD) for time-frequency analysis of EEG signals and then combined improved sample entropy and phase synchronization indices as features to distinguish seizure from non-seizure activity [5]. The accuracies of these algorithms mainly depend on the capacity to recognize features distinguishing different types of EEG signals.

Gaussian Mixture Models (GMMs) yield stable mean vector and covariance matrix distributions for reliably describing signal characteristics [6]. The covariance matrix is an important tool to describe the correlation between features, which has been studied in many fields for time series [7]. Mean vectors of GMMs are also important in EEG and image classification [8], [9]. Patnaik et al. completed the work of time-frequency decomposition of EEG signals using wavelet decomposition, and then calculated the average value of wavelet coefficients and completed the classification of EEG signals using feedforward back propagation artificial neural network (ANN) [10]. The space of the Gaussian distribution in the GMMs is not linear, but rather a smooth Riemannian manifold. In this paper, we indirectly mapped Gaussian distributions to Euclidean space via logarithmic mapping and then processed the GMMs using simple Euclidean operations.

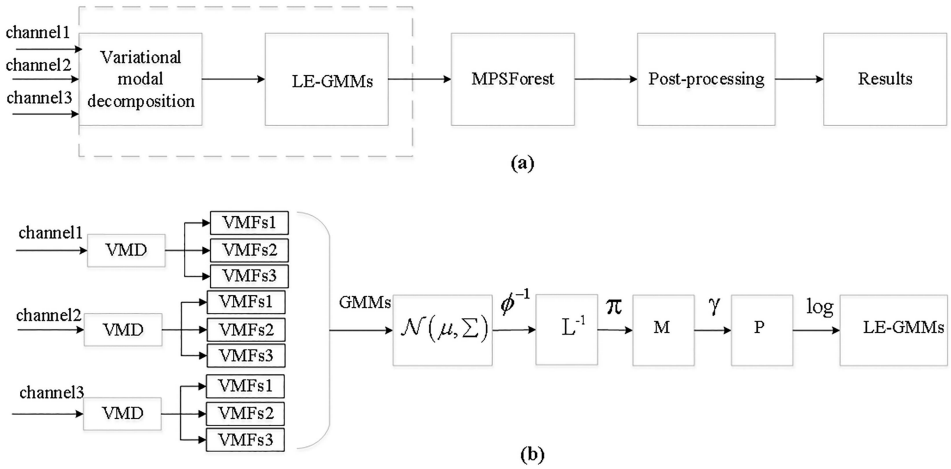

Fig. 1. Block diagram of the flow of the proposed seizure detection algorithm. (a) The complete structure of the detection process, including preprocessing based on variational mode decomposition, feature extraction by LE-GMMs, classification, and post-processing. (b) The details of processing demarcated by the dashed box in (a), including VMD preprocessing and computation of LE-GMM features, where ϕ^{-1} represents the inverse of the Cholesky decomposition, π is the left polar decomposition, γ is the bijective function, and log represents the log-Euclidean frame.

Deep learning algorithms are growing in popularity for digital and image signal classification due to its greater accuracy than traditional machine learning methods [11]. Convolutional neural networks (CNN) are an important component of deep learning models that have been applied to seizure detection. Wei et al. proposed a 12-layer CNN model combined with a merger of the increasing and decreasing sequence (MIDS) to increase the distinguishing characteristics for epilepsy detection [8].

Deep Forest is a novel deep learning model based on the deep neural network approach [12]. The model is composed mainly of cascade forests and multi-granularity scans and uses sliding windows to enhance the connections among features [13]. The structure of a cascade forest is similar to that of a neural network, but the difference is that each node of a cascade forest is a random forest rather than a neuron. In addition, deep forests have fewer parameters than neural networks, and the same parameters perform well for different applications. For instance, Cheng et al. designed a multi-channel EEG emotion recognition system utilizing 2D frame sequences and deep forests that greatly reduced the complexity of recognition [14], while Zhou et al. combined the binary and deep forest generated by the hash algorithm to achieve image classification [15] and Liu et al. proposed a micro-RNA (mi-RNA) disease association prediction method combining autoencoders and deep forests [16].

Moreover, several studies also have identified potential deficiencies of deep forests and made improvements. Guo et al. proposed a BCDForest model to deal with the problem of classifying cancer subtypes in small biological datasets. In their work, multiple simple binary classifiers are trained by using the entire training data to encourage ensemble diversity, and a boosting strategy is also introduced to emphasize the important features in the cascade forest to improve the classification performance [17]. Siamese Deep Forest is another modified deep forest model developed by Utkin et al., which used a modified training set consisting of concatenated pairs of vectors and defined the class distributions in the deep forest as the weighted sum of the tree class probabilities to prevent overfitting [18]. Since the seizure detection system needs both good accuracy and high speed, we propose the Multi-Pooling and error Screening Forest (MPSForest) based on the deep forest model, which has the advantages of smaller memory requirements and better classification performance than traditional deep forests. MPSForest mainly includes multi-pooling, error screening and class vector stacking to strengthen the recognition ability of the deep forest model on EEG signals.

The purpose of this study is to propose an innovative algorithm for automatically detecting seizure activity from EEG signals. The main contribution of this work could be summarized as follows:

- LE-GMMs are proposed to describe the high-order characteristics of EEG signals and exploit the capacity of GMMs to distinguish non-seizure and seizure data, which preserves the algebraic and geometric structure of GMMs by mapping the spatial structure of GMMs from Riemannian manifolds to Euclidean space.
- Based on the traditional deep forest, MPSForest introduces the multi-pool and OOB error screening mechanism to enhance the detection accuracy and reduce the computational burden.
- The preprocessing with VMD could help to obtain useful EEG information and the post-processing techniques also optimize the accuracy of seizure detection.
- This algorithm was evaluated using two EEG datasets with 29 patients and achieved competitive results compared with other recent studies using the same datasets.

The remaining chapters of this paper are structured as follows: Section II describes two EEG databases, and Section III describes preprocessing, feature extraction, classification, and post-processing steps. The experimental results and parameter settings are then summarized in Section IV. The discussion and conclusion are presented specifically in Section V and Section VI.

II. EEG Datasets

A. Freiburg EEG Dataset

This EEG dataset used to construct and test our proposed model was obtained from the University Hospital Freiburg, Germany. The long-term Freiburg dataset includes the intracranial EEG signals from 21 patients differing in age, type of seizure, duration of seizure, location of seizure, and number of seizures. Both males and females are included in roughly equal frequency. Further, it is one of the most popular datasets used for automatic epilepsy detection and prediction modeling [19], [20].

The sampling frequency of all data for the 21 patients was 256 Hz. Highly experienced neurologists selected six channels for each patient according to EEG characteristics, three from the focal areas and three from extra-focal areas. Only three channels in the focal areas were studied in the current work. The duration of seizure activity varies among patients according to type and etiology. Long seizures were defined as those greater than 10 minutes, while short seizures were defined as those lasting only a few seconds. Individual patient EEG recordings captured two to five seizure events. Authoritative clinical research experts determined seizure start and end times based on EEG records and clinical manifestations. Overall, the Freiburg dataset contains 87 seizure events averaging 114.3 s in duration. A more detailed description of the Freiburg dataset can be found in a previous report [19].

For the current study, we randomly selected a non-seizure period and one or more epileptic seizure events as the training set, and the rest of the data served as the testing set to validate the performance of the algorithm. The training set contained 83.35 minutes of seizure activity from 34 individual seizure events and 3.6 hours of non-seizure activity, while the test set consisted of 1.95 hours of seizure activity from 53 individual seizure events and 648.57 hours of non-seizure activity.

B. UPenn and Mayo Clinic's Seizure Detection Challenge Dataset

The UPenn and Mayo Clinic's Seizure Detection Challenge dataset includes intracranial EEG recordings of four dogs and eight patients [21]. The EEG recordings of the four dogs were sampled by 16 electrodes at 400 Hz, whereas the human EEG recordings were acquired by the different number of electrodes sampled at 500 Hz or 5000 Hz. All of the data were pre-segmented into 1s EEG segments and labeled as "seizure" or "non-seizure". In this paper, our model will be tested using the EEG recordings of all eight patients.

III. Methods

The seizure detection algorithm is explained schematically as shown in Fig. 1. The detection process consists of four steps: preprocessing based on variational mode decomposition, feature extraction by LE-GMMs, MPSForest classification, and post-processing, which are displayed in each block of Fig. 1(a). Specifically, variational modal decomposition (VMD) is carried out for the adaptive time-frequency analysis of EEG signals and reducing noise artifacts effectively, which lays a good foundation for the following feature extraction. Then the GMMs are applied to represent the time-frequency distribution of EEG, and the LE-GMMs are constructed as the EEG feature by indirect mapping to embed the Riemannian manifold into Euclidean space, as presented in Fig. 1(b). The extracted features are sent to the proposed MPSForest for classification. Finally, post-processing techniques including smoothing, threshold judgment and adaptive collar technique are implemented to improve detection accuracy. Each process would be described in detail below.

A. Preprocessing Based on Variational Mode Decomposition

Electroencephalographic signals are non-stationary and dynamic, so the recorded EEG signals were first divided into 4-s epochs using a sliding non-overlapping window to create relatively stable individual units long enough to capture seizure activity but brief enough to clearly distinguish seizure and non-seizure activity.

Variational mode decomposition (VMD) is a completely non-recursive state time-frequency decomposition method appropriate for the analysis of nonlinear and non-stationary EEG signals [22]. The core idea of VMD is the adaptive decomposition of the original signal into a series of variational mode functions (VMFs) around the constantly changing center frequency. In contrast to other methods like empirical mode decomposition (EMD) that continuously filter and obtain intrinsic modal functions (IMFs), VMD adaptively obtains the VMFs by finding the optimal solution of the constrained variational model. Below we describe VMFs construction and solutions for EEG data using VMD.

For the raw EEG signal $f(t)$, it is decomposed into non-recursive modes $u_k, k = 1, 2, \ldots, K$, that is VMFs. Each mode can be expressed as follows:

$$u_k = A_k \cos(\phi_k) \tag{1}$$

here, A_k is the envelope of VMF and ϕ_k is the phase. The derivative of the phase is the central frequency ω_k, $\omega_k = \phi'_k$ where the VMFs is centered on it. We constructed the constrained variational mode model through the following three steps. (1) We calculated the one-sided spectrum of each VMFs using the Hilbert transform. (2) The hybrid index term was then used to map each VMFs to the corresponding center frequency baseband. (3) Finally, we calculated the bandwidth of each VMFs by combining the Gaussian smooth demodulation signal. The constructed constrained variational model can be expressed as:

$$\begin{aligned} &\min_{\{u_k\},\{\omega_k\}} \left\{ \sum_k \left\| \partial_t [(\delta(t) + j/\pi t) * u_k(t)] e^{-j\omega_k t} \right\|_2^2 \right\} \\ &\text{s.t.} \sum_{k=1}^{K} u_k = f \end{aligned} \tag{2}$$

Then, the optimal solution of the constrained optimal model was calculated, and the penalty factor α and Lagrange multiplier λ are used to form the augmented Lagrange(L) , so as to realize the transformation of the constrained variational problem to the

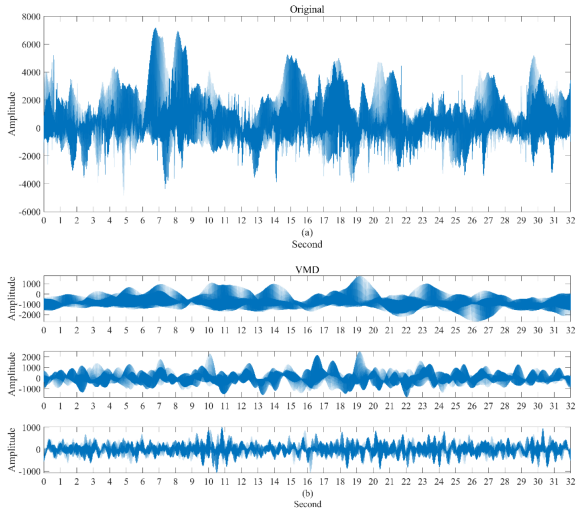

Fig. 2. A section of original EEG recording during the seizure period and the sub-signals decomposed using VMD. (a) Original signals; (b) Sub-signals decomposed by VMD (VMF1, VMF2, VMF3).

unconstrained variational problem.

$$L(\{u_k\},\{\omega_k\},\lambda)=\alpha\sum_k\left\|\partial_t[(\delta(t)+j/\pi t)*u_k(t)]e^{-j\omega_k t}\right\|_2^2$$
$$+\left\|f(t)-\sum_k u_k(t)\right\|_2^2+\langle\lambda(t),f(t)-\sum_k u_k(t)\rangle \quad (3)$$

The original signal was decomposed into a series of VMFs by first decomposing low-frequency information useful for seizure detection and then decomposing high-frequency information. In this study, we set the number of modes for decomposing the original signal to $k=5$. To reduce the interference of high-frequency information, the first three layers containing rich low-frequency seizure information were selected as sub-signals. Fig. 2 compares the raw EEG signal with the decomposed sub-signals VMF1, VMF2, and VMF3 when $k=5$.

B. Feature Extraction By Logarithmic Euclidean-Gaussian Mixture Models

Gaussian Mixture Modeling is a clustering method suitable for describing the multimodal distribution of EEG signals [9], [23]. The Gaussian distribution is located in a Riemannian manifold. If only the Riemannian manifold structure modeled by the GMMs is considered, subsequent calculations are complex, limiting the utility off Gaussian distribution modeling. Therefore, we propose LE-GMMs that indirectly embed the Gaussian distribution of GMMs in a linear space. This method allows simple linear operations while preserving the Riemannian manifold structure of the Gaussian distribution, greatly reducing the computational burden.

It is well known that the covariance matrix $\sum$ in GMMs is symmetric positive definite (SPD), and each SPD matrix has a unique Cholesky decomposition ϕ , which can be decomposed into the product of a positive definite lower triangular matrix and its transposed matrix [24]. The positive definite lower triangular

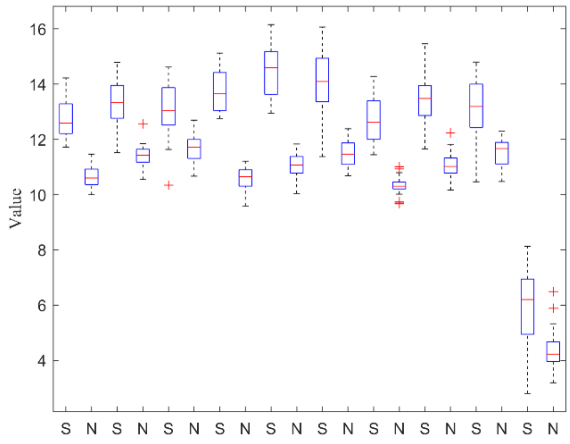

Fig. 3. Boxplot of diagonal elements of LE-GMMs. “S” represents the seizure period and “N” denotes the non-seizure period.

matrix has an inverse function ϕ^{-1} , which can map the Gaussian distribution $N(\mu,\sum)$ to an upper triangular matrix L^{-1} so that the diagonal elements are all positive numbers and the last element is 1.

$$\phi^{-1}:\sum=L^{-T}L^{-1} \quad (4)$$

For any positive determinant matrix, L^{-1} has a unique left pole decomposition π ,

$$\pi:L^{-1}=MR \quad (5)$$

$$M=\sqrt{L^{-1}L^{-1^T}}=\begin{bmatrix}\sum+\mu\mu^T & \mu\\ \mu^T & 1\end{bmatrix}^{\frac{1}{2}} \quad (6)$$

$$R=\arg\min\left\|L^{-T}-O\right\| \quad (7)$$

where $\|\cdot\|$ is the Frobenius norm, O is an orthogonal group, and M is a Lie group structure. There is a bijective function γ that can map M to P, thereby transforming the spatial structure to a symmetric positive definite matrix space

$$\gamma:M\to P. \quad (8)$$

The fourth mapping function log uses the logarithm-Euclidean framework to convert the Riemann operation in real symmetric positive definite space into a Euclidean operation in linear space through the matrix logarithm operation [25].

$$\log:P\to\log(P) \quad (9)$$

The matrix $P_{x,y}$ obtained by mapping the four functions is still an SPD matrix. We extracted the diagonal elements and formed vector LE-GMMs by column.

$$\text{LE-GMMs}=[P_{11},P_{22},P_{33},\ldots,P_{nn}] \quad (10)$$

In this study, after applying the VMD to obtain the time-frequency EEG matrixes, we calculated the GMMs of EEG epochs where the number of Gaussian components was set to 3. The spatial structure of the Gaussian mixture models was mapped from a Riemannian manifold to the Euclidean space by LE-GMMs. This method not only retains the algebraic and geometric structure of the GMMs, but also allows GMM processing with the simple Euclidean operations. As shown

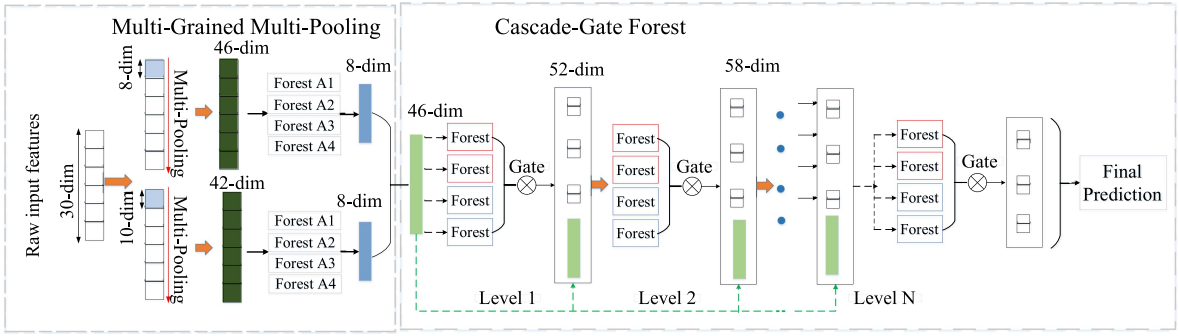

Fig. 4. Flowchart of the complete framework of the MPSForest structure. Multi-pooling denotes max pooling and average pooling.

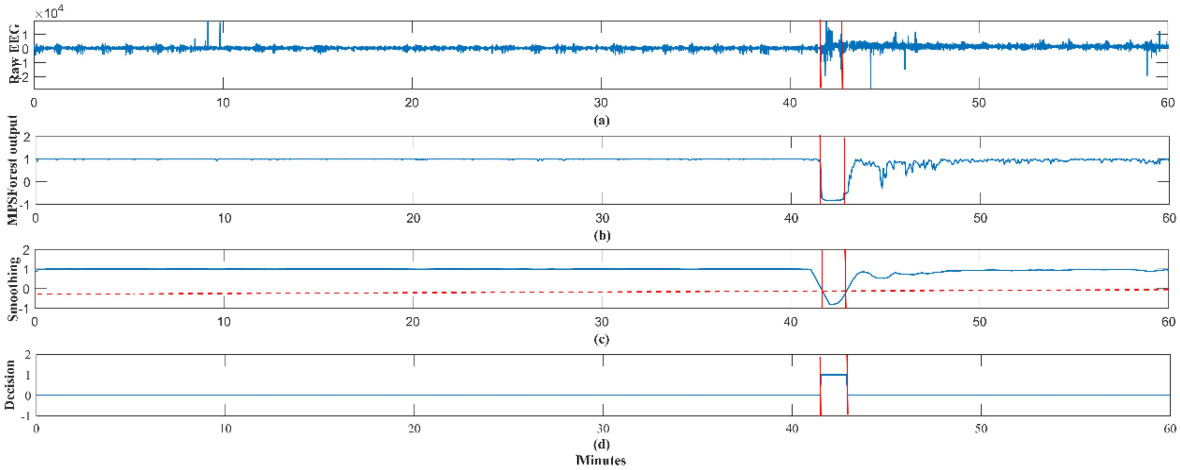

Fig. 5. Example of a seizure event successfully detected in patient 20 using the complete post-processing technology. (a) The raw 1-h EEG record of patient 20. (b) Probability output of the MPSForest. (c) Smoothed probability output after moving average filtering. The threshold value is represented by the red dotted line. (d) The binary judgment following the collar technique, where the expert-marked epileptic seizure duration is indicated by the space between the two red vertical lines.

TABLE I
CENTRAL FREQUENCIES YIELDED BY DIFFERENT MODAL FUNCTION NUMBERS FROM THE FREIBURG DATABASE

Number of modes	Center frequency					
2	0.0042	0.0645	—	—	—	—
3	0.0031	0.0447	0.1349	—	—	—
4	0.0029	0.0405	0.1003	0.1940	—	—
5	0.0029	0.0395	0.0937	0.1728	0.3399	—
6	0.0025	0.0521	0.1092	0.1814	0.3553	0.0347

in Fig. 3, a statistical analysis of the LE-GMMs boxplots indicated significant differences in the distribution of seizure and non-seizure EEG data.

C. Multiple Pooling and Error Screening Forest Classification

Deep Forest is an ensemble model based on deep neural networks with multi-granularity scanning and cascaded forest structure [12]. Multi-granularity scanning uses sliding windows to enhance the correlations among features, and the cascading forest adopts a layer-to-layer mode to learn input features. Unlike DNN using complex forward and backward propagation algorithms to learn hidden variables, cascade forest learning combines random forest learning methods to distinguish the distribution of different kinds of vectors. Compared with traditional classifiers and deep neural network algorithms, the tree-based deep forest model is easier to adjust parameters and performs well in the field of small sample classification, while retaining the ability of deep feature learning.

However, the original deep forest model transforms the original features into a large number of sub-features after multi-granularity scanning, consuming a lot of memory and time. Therefore, we employed a multi-pooling process on the multi-granularity scanning, which is analogous to feature pooling in convolutional neural networks [26], [27].

In addition, the random forest will randomly select some irrelevant features when constructing the tree, affecting the sensitivity of each decision tree and the overall performance of the algorithm, especially using small-sample datasets. To solve this problem, we proposed a cascade-gate forest based on an out-of-bagging (OOB) error screening mechanism and a stack of class vectors, analogous to the gates in Long Short-Term Memory networks (LSTM) [28]. Therefore, an improved deep forest model with Multiple Pooling and error Screening Forest (MPSForest) is constructed as shown in Fig. 4, which consists of multi-granularity multi-pooling and cascade-gate forest.

Combining max and average pooling while preserving multi-granularity scans, seizure features can be highlighted, the distinctions between seizure and non-seizure activity can be enhanced, and the dimension of the data can be reduced, thereby greatly reducing memory load and computation time. Using an out-of-bagging (OOB) error screening mechanism, the method obtains the class vector of each random forest from the cascaded class vectors [29].

The features after the granularity scanning will generate the class vector of the sample x when it passes through the cascade forest

$$P^{(t,f)}(x) = (P_1^{(t,f)}(x), P_2^{(t,f)}(x), \ldots P_c^{(t,f)}(x)) \tag{11}$$

where $P^{(t,f)}$ is the class distribution of each decision tree.

The class distribution vector $V^{(t,f)}$of each tree is obtained by calculating the mean probability of its class distribution

$$V^{(h,t,f)}(x) = (V_1^{(h,t,1)}(x), V_2^{(h,t,2)}(x), \ldots V_c^{(h,t,f)}(x)) \tag{12}$$

The parameter s was then used to calculate the class vector with the largest OOB error and filter to obtain a new class vector

$$V^{(h,t,f,s)}(x) = (V_1^{(h,t,1,s)}(x), V_2^{(h,t,2,s)}(x), \ldots V_c^{(h,t,f,s)}(x)) \tag{13}$$

where s represents the ratio of the class vector to be filtered. As shown in Fig. 4, the input of the cascade-gate forest is composed of the class vector output by the previous layer and the original feature vector.

As the number of cascaded layers increases, the information carried by the original features will gradually be hidden, which will influence classification. To avoid this situation, the input of the cascade-gate forest was changed to the output class vector and the original feature vector stack OOB was filtered in the previous layer as described by

$$I^{(h,t,f)}(x) = (O^{(1,t,f)}(x), O^{(2,t,f)}(x), \ldots O^{(h-1,t,f)}(x), V_{ini}) \tag{14}$$

where $I^{(h,t,f)}$is the input vector of the h layer, $O^{(h-1,t,f)}$ is the output vector of the level $h-1$ layer, and V_{ini} is the initial input feature vector. In this study, the parameter s was set to 0.25. Finally, we determined the predictions for the two different types of EEG signals using the mean class probability of the last layer of the cascade-gate forest.

For the Freiburg dataset, after the LE-GMMs features were extracted, they were sent into the proposed MPSForest model and the dimension of features for one EEG segment is 30. In the multi-grained multi-pooling scanning phase, the windows of multi-granularity scans were set to 8 and 10. Thus, the window of size 8 was used to scan 30-dimensional raw features in turn, and the max-pooling and average-pooling were performed on the feature segments after scanning to construct a 46-dimensional vector. Similarly, the window of size 10 was used to scan the original features and generate 42-dimensional data after multi-pooling. These data were trained on two full random forests and two random forests and got an 8-dimensional class vector, respectively. The two 8-dimensional class vectors were concatenated with the original feature vector to form a 46-dimensional vector as the input of the cascade-gate forest. In the cascade-gate forest phase, the 46-dimensional original vector is trained in the first-level four forests of the cascade forest to generate four class vectors. Then, based on the out-of-bagging (OOB) error screening, one class vector was filtered out and the remaining ones were combined with the original input vector to form a 52-dimensional vector to be sent into the second-level forests. The same procedure is executed until the last level yields three pairs of class vectors and finally a 2-dimensional class probability was obtained using the average value of these three class vectors.

D. Post-Processing

To increase the accuracy of MPSForest output, post-processing procedures were carried out. These included output probability difference, smoothing, threshold comparison, and adaptive collar technology. Two probabilities obtained by the MPSForest model were used to classify seizure and non-seizure EEG epochs, and the difference between the two probabilities was defined as the final judgment probability. The moving average filter (MAF) was first applied to the output of the MPSForest to lessen the random noise and eliminate any potential errors brought on by the noise [30]. Despite being the most basic low-pass filter, MAF provides exceptional smoothing capabilities that help detect epilepsy by successfully removing the influence of noise while preserving the distinguishing characteristics needed for seizures. The MAF is defined as

$$y_k = \frac{1}{2M+1} \sum_{i=-M}^{M} \hat{y}_{k+i} \tag{15}$$

where $\hat{y}$ denotes the probabilistic output, y is the filtered signal, and $2M+1$ is the smoothing length. Then, each patient was assigned a threshold, and epochs with probabilities y_k greater than this threshold were classified as seizure and marked as "1", while epochs with probabilities below the threshold were classified as non-seizure and marked as "0".

Furthermore, because seizure activity is a dynamic and continuous process in each patient, the EEG features at the beginning and end of a seizure are often not very different from those of the non-seizure period. To address this limitation, we employed an

TABLE II
COMPARISON OF CLASSIFICATION RESULTS FOR THE FREIBURG DATASET USING OUR ALGORITHM AND OTHER MODELS

Authors	EEG data duration/h	Number of patients	Sensitivity(%)	Specificity(%)	Accuracy(%)	False detection rate/h
Zhou et al. [33]	-	21	93.7	97.2	95.4	-
Mahmoodian et al. [34]	560	19	95.83	96.70	96.84	0.24
Tzimourta et al. [35]	28.6	21	99.74	97.30	97.74	0.21
Liu et al. [36]	720	21	97.01	98.12	98.12	0.36
Li et al. [37]	564	21	97.47	96.17	96.17	0.48
Abugabah et al.[38]	150	10	99.1	99	98.9	-
Hussain et al. [39]	-	21	94.71	93.59	90.53	-
Mu et al. [40]	559	21	93.20	98.16	98.16	0.50
Shoeibi et al.[19]	-	21	99.54	99.56	99.28	-
Yuan et al. [41]	590	21	96.48	98.56	98.55	0.44
Our works	655.3	21	98.47	98.78	98.77	0.24

TABLE III
EPOCH-BASED EVALUATION RESULTS IN THE FREIBURG DATASET

Patient	Sensitivity	Specificity	Accuracy	G-mean	$F1_{weighted}$
1	87.50	99.44	99.44	93.27	0.9969
2	100	99.43	99.43	99.71	0.9961
3	100	99.00	99.00	99.49	0.9931
4	100	99.25	99.25	99.62	0.9947
5	100	99.26	99.26	99.63	0.9943
6	100	99.97	99.97	99.98	0.9997
7	100	97.97	97.97	98.97	0.9845
8	100	95.23	95.23	97.59	0.9790
9	100	96.32	96.32	98.14	0.9778
10	98.55	97.22	97.12	97.88	0.9830
11	100	99.95	99.95	99.97	0.9996
12	100	99.82	99.82	99.71	0.9988
13	100	98.94	98.94	99.46	0.9929
14	100	98.10	98.10	99.05	0.9816
15	100	98.47	98.47	99.23	0.9871
16	100	98.30	98.30	99.10	0.9885
17	100	99.91	99.91	99.95	0.9983
18	81.81	99.44	99.34	90.20	0.9963
19	100	99.14	99.14	99.57	0.9954
20	100	99.39	99.39	99.69	0.9954
21	100	99.82	99.82	99.91	0.9964
Mean	98.47	98.78	98.77	98.57	0.9919

TABLE IV
EVENT-BASED EVALUATION RESULTS IN THE FREIBURG DATASET

Patient	Number of seizures marked by experts	Number of seizures detected by our system	Event-based sensitivity	False detection rate/h
1	2	2	100	0.4
2	1	1	100	0.13
3	3	3	100	0.16
4	3	3	100	0.09
5	3	3	100	0.19
6	2	2	100	0.03
7	2	2	100	0.62
8	1	1	100	0.70
9	3	3	100	0.47
10	3	2	67	0.35
11	2	2	100	0.06
12	3	3	100	0.27
13	1	1	100	0.25
14	3	3	100	0.20
15	2	2	100	0.13
16	3	3	100	0.25
17	4	4	100	0.10
18	3	2	67	0.21
19	2	2	100	0.33
20	3	3	100	0.13
21	4	4	100	0.06
Total	53	51	96.2	0.24

adaptive collar technique to extend the detected seizure events by n epochs both at the beginning and at the end [31]. Fig. 5 shows an example of a seizure event successfully detected in patient 20 using all of the post-processing technical steps described.

IV. RESULTS

A. Evaluation Criteria

This seizure detection algorithm was implemented in python3.7 and Matlab 2018a environments. In this experiment, we used both epoch-based and event-based evaluation criteria to distinguish seizure and non-seizure data. The five main epoch-based evaluation indicators were sensitivity, specificity, accuracy, G-mean and weighted F1-score, which are defined as:

$$\text{Sensitivity} = \frac{TP}{TP + FN} \tag{16}$$

$$\text{Specificity} = \frac{TN}{TN + FP} \tag{17}$$

TABLE V
EPOCH-BASED EVALUATION RESULTS IN THE UPENN AND MAYO CLINIC'S SEIZURE DETECTION CHALLENGE DATASET

Patient	Sensitivity	Specificity	Accuracy	G-Mean	$F1_{weighted}$
Pat 1	98.54	100	99.21	99.27	0.9941
Pat 2	100	99.52	99.52	99.75	0.9955
Pat 3	95	98.79	98.25	96.87	0.9874
Pat4	100	100	100	100	1
Pat 5	97.92	99.54	98.63	98.72	0.9946
Pat 6	99.82	98.72	99.11	99.26	0.9884
Pat7	99.23	97.14	97.68	98.17	0.9747
Pat 8	95.25	98.27	94.26	96.74	0.9802
Mean	98.22	98.99	98.33	98.59	0.9894

$$\text{Accuracy} = \frac{TP + TN}{TP + FP + TN + FN} \tag{18}$$

$$G - \text{mean} = \sqrt{\text{Sensitivity} * \text{Specificity}} \tag{19}$$

Here, sensitivity reflects the capacity of the algorithm to detect seizures, specificity reflects the capacity to detect non-seizure periods, and G-mean is a metric for overall classification performance. In addition, F1-score is also an important criterion to measure the accuracy of the classification model by taking the recall and precision into account, which is calculated traditionally as follows:

$$\text{F1} = \frac{2TP}{2TP + FP + FN} \tag{20}$$

But when there is a large difference in the amount of data between the two classes of seizures and non-seizures, we need to consider the performance of all the classes, so the weighted F1-score is used in this work, which is defined as:

$$\text{F1}_{weighted} = P_{seizure} \times F1_{seizure} + P_{non-seizure} \times F1_{non-seizure} \tag{21}$$

where $P_{seizure}$ is the proportion of seizure samples to the total samples, while $P_{non-seizure}$ is the proportion of non-seizure samples, $F1_{seizure}$ is the F1-score using the seizure data as the positive class, and $F1_{non-seizure}$ is the F1-score using the non-seizure data as the positive class.

The event-based sensitivity and false detection rate are two event-based evaluation metrics. The event-based sensitivity is calculated by dividing the total number of seizures identified by experts by the number of actual seizures detected by the algorithm. The false detection rate was established as the typical number of erroneous detections per hour, and the algorithm treats one or more consecutive false positives as a false detection.

B. Experimental Results

The detailed epoch-based and event-based results for the two EEG datasets can be found in Tables III, IV and V. The evaluations of the 21 patients in the Freiburg dataset, conducted using epoch-based and event-based methodologies, are shown in Tables III and IV, respectively. The epoch-based classification produced good results, as shown in Table III, with a sensitivity of 98.47%, specificity of 98.78%, the accuracy of 98.77%, G-mean of 98.57%, and weighted F1-score of 0.9919. The epoch-based method yielded perfect sensitivity of 100% for 18 patients (patients 2–9, 11–17, 19, 20, and 21) and specificity above 99% for more than half of the patients with specificity below 97% for only two patients (patients 8 and 9). Further, the G-mean exceeded 99% for 15 patients and was below 97% for only two patients (patients 1 and 18), both of which had very short seizure durations limiting the identification of effective distinguishing features.

Event-based evaluation criteria have greater practical applicability for clinical medicine. In our experiments, a set consisting of 34 seizure events and a series of corresponding non-seizure epochs were used to train the classification model, while the remaining 53 seizure events and the remaining non-seizure recordings were used to test the algorithm. Table IV shows that just two of the 53 seizure events were not recognized, indicating that the mean event-based sensitivity was 96.2%. 21 patients had false detection rates that were all less than 1/h, with the mean false detection rate being 0.24/h. The highest false detection rate was recorded by patient 8, which was 0.7/h.

The epoch-based evaluation results of the 8 patients in the UPenn and Mayo Clinic's Seizure Detection Challenge dataset are shown in Table V. The average sensitivity, G-mean, accuracy and specificity were 98.22%, 98.59%, 98.33%, and 98.99% respectively. The average weighted F1-score is 0.9894. Patient 4 achieved 100% on all five indicators. It can be inferred that our proposed method has good performance in EEG classification and seizure detection and a larger EEG dataset would be applied to further verify and improve our algorithm in future work.

C. Parameter Setting in VMD

The core electrophysiological signature of seizure activity is the emergence of large amplitude spikes and waves that are absent during normal cortical activity, so it is possible to detect seizures automatically using time-frequency analysis. The VMFs of the VMD decomposition are inextricably linked to the central frequency. Moreover, the VMD decomposition always decomposes the low-frequency information that contributes to seizure detection first, and then decomposes the interfering high-frequency information, so the central frequency of each VMF must be increasing. Table I shows the central frequency distribution of EEG recordings from the Freiburg dataset using different modal numbers k. It can be seen that the central frequency does not increase continuously when $k = 6$, indicating that there is an over-decomposition at this point. Therefore, it is important to choose the appropriate number and we choose the number of modes $k = 5$.

Moreover, choosing the appropriate number of layers after VMD decomposition is also critical since the excessive increase in the number of layers can result in a spurious VMF. To eliminate the effect of spurious VMFs, the correlation coefficient between each VMFs and the original EEG signal was computed. The correlation numbers of VMF1 to VMF5 with the original signals were 0.8598, 0.5298, 0.3105, 0.1813, and

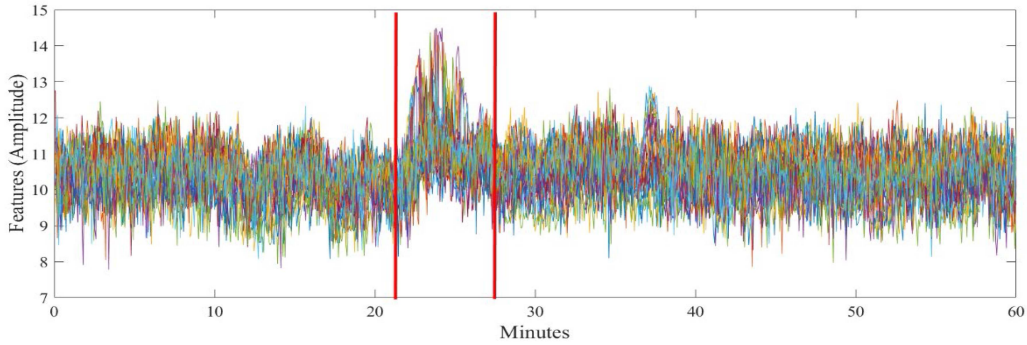

Fig. 6. Extracted LE-GMMs features for 1 h EEG data containing one seizure event in Freiburg dataset, the two red vertical lines represents seizure data.

0.0773, respectively, while the correlation coefficients of VMF4 and VMF5 were less than 0.3, indicating that they contain less information that contributes to seizure detection. To improve the validity of our model, we only kept VMF1, VMF2 and VMF3 as effective sub-signals for feature extraction.

V. Discussion

Achieving both high sensitivity and specificity requires reliable distinguishing features. Our method uses LE-GMMs to identify EEG differences between seizure and non-seizure states. Seizure is a dynamic process from the onset to the final end, and the corresponding EEG signal characteristics are also subject to dynamic changes. Despite fluctuations, multiple EEG characteristics can distinguish seizure activity from non-seizure activity. Fig. 6 shows the extracted LE-GMM features for 1-h EEG signals containing one seizure event and it can be seen that the extracted features fluctuated continuously, but there are still significant differences between the seizure and non-seizure stages.

The covariance matrix in Gaussian mixture models is an important seizure descriptor because it reflects the second-order statistical characteristics of the signal and describes multiple parameters and correlations. Based on the method of local log-Euclidean covariance matrix in [32], we proposed the logarithmic Euclidean covariance matrix (LECM) as a valid EEG feature, which is a map of the covariance matrix in the log-Euclidean framework, and made a comparison with LE-GMMs. The internal covariance matrix and mean vector of LECM are always fixed, while LE-GMMs use Gaussian mixture models for signal high-order statistics. Therefore, LE-GMMs can capture a greater number of information-rich EEG characteristics. Fig. 7 shows the comparison of detection results for LECM and LE-GMMs under the MPSForest model. It can be seen from Fig. 7 that the average sensitivity, specificity, accuracy, and G-mean in the Freiburg dataset are higher using LE-GMMs than LECM.

Deep neural networks are frequently used for epilepsy detection. These networks pool layers to reduce dimensions, highlight important features, and greatly reduce the running time of the algorithm. The proposed MPSForest not only has the processing characteristics of deep neural network, but also has the structure of random tree and the multi-pool and OOB error screening

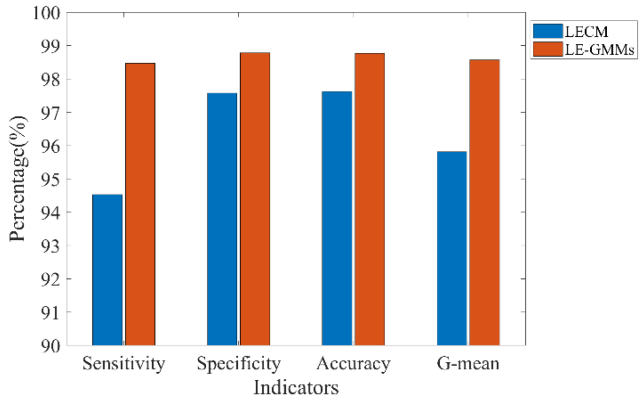

Fig. 7. Comparison of LECM and LE-GMM detection results using the MPSForest model.

mechanisms. But selecting the optimal pooling methods is also critical. Fig. 8 is a comparison of the classification results of 21 patients in the Freiburg dataset under the same input with the Mean-Max pooling method proposed in the current study and three other pooling methods (Non-pooling, Mean pooling, and Max pooling). It can be seen that our algorithm is superior to other pooling methods, and has stronger robustness and applicability.

In addition, the EEG recordings were broken into fixed-length segments and the VMD divided the EEG signals into various scales to create the EEG distributions during the preprocessing stage. These operations provided the diversity of seizures in abundant frequency bands and removed the high-frequency components from the EEG data. What's more, we did not simply use threshold judgment after the MPSForest model, but also increased the smoothing filter and the adaptive collar operation in order to further reduce the possibility of the error caused by sporadic oscillations and more precisely find the seizure. In general, it is the combination and cooperation of each step that can result in an automatic epilepsy detection system with good performance.

The Freiburg dataset has been used to validate the epilepsy detection algorithm in many works. A comparison of our results with other research using the Freiburg EEG dataset is presented in Table II. Zhou et al. used the frequency domain information of

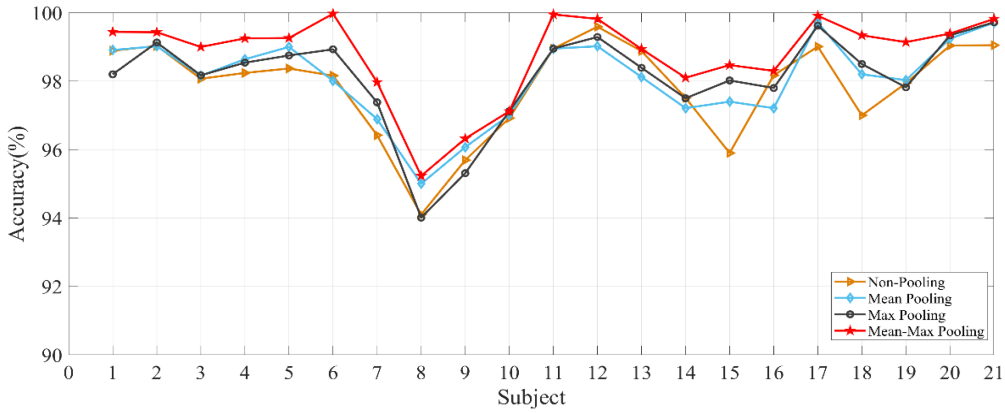

Fig. 8. Classification accuracy of Deep Forest by Non-pooling, Mean pooling, Max pooling, and Mean-Max pooling when the input features are LE-GMMs.

the original EEG signal and convolutional neural network to realize the identification of epileptic seizures and non-seizures[33]. The sensitivity, specificity, and accuracy of their method are only 93.7%, 97.2%, and 95.4%, which were lower than our work. In addition, Mahmoodian et al. proposed an automatic epilepsy detection model combining cross-bispectral features and support vector machines [34]. In their study, they achieved a low false detection rate of 0.24/h, but they only trained 19 patients, ignored 8 and 13 patients, and the total EEG duration was only 560 h. Therefore, the current model yields slightly greater accuracy and may be more broadly applicable, at least for patients with seizure activity lasting more than several seconds.

The model of Tzimourta et al. distinguished seizure from non-seizure activity by extracting energy, entropy, mean, standard deviation, and variance of sub-band coefficients as categorical features and then constructing a random forest decision model [35]. Although the epoch-based sensitivity of their model was higher than ours, the model missed two seizures in patient 1 and one seizure in patient 7. Further, they used only 28.6 h of EEG recordings as testing data. Liu et al. proposed the detection algorithm using the Stockwell transform and a 15-layer CNN [36]. Although the duration of testing EEG data was longer than our study, their accuracy was slightly lower and the mean false positive rate higher. Li et al. proposed a nested long and short-term memory algorithm to achieve automatic seizure detection [37], which learned the distinction between seizures and non-seizures through a fully convolutional network of three convolutional blocks and finally completed the classification under the NLSTM model. The method of Abugabah et al. achieved 98.9% accuracy on patients 1–10 of the Freiburg dataset by screening 15 statistical features and using an artificial algae optimization neural network [38].

Recently, Hussain et al. proposed a deep learning hybrid model with a combination of CNN and LSTM [39]. They directly put the temporal information of EEG signals into the deep learning hybrid model to achieve classification, eliminating the step of feature extraction. In the work of Mu et al., the discrete wavelet decomposition, graph-regularized non-negative matrix factorization (GNMF) and BLDA classifier were combined to automatically detect epileptic seizures, which yielded 93.20% sensitivity and 0.50/h false detection rate [40]. The results of these two studies are all lower than our algorithm. Shoeibi et al. used autoencoders, fuzzy entropies and ANFIS classifier to present a novel seizure diagnostic procedure, and obtained an accuracy of 99.28% on the Freiburg dataset [19]. Although their results are better than ours, the EEG data duration used in their paper is not explained, which makes us unable to make more specific comparisons. Moreover, in our previous work, we combined GNMF and kernel-based robust probabilistic collaborative representation (ProCRC) for seizure detection [41], which achieved a false detection rate of 0.44/h.

For the UPenn and Mayo Clinic's Seizure Detection Challenge dataset, Yıldız et al. proposed a fully-unsupervised deep learning method for seizure identification using a variational autoencoder (VAE), which eventually achieved an average accuracy of 79% [42]. Zhao et al. proposed a multi-layer weighted self-learning algorithm on seizure detection and obtained an F1 score of 0.84, which was not as good as ours [43].

Collectively, these findings indicate that multiple distinct computational strategies can distinguish seizure from non-seizure activity in EEG recording with acceptable accuracy. Among these strategies, however, the model proposed here demonstrates superior overall accuracy. Additional studies are needed to determine if this model also has superior generalizability, such as the capacity to distinguish between three or more types of EEG activity.

VI. Conclusion

In this work, an effective system applying LE-GMMs and MPSForest model is proposed for epileptic seizure detection. GMMs contain high dimensional statistical properties and could well approximate EEG multimodal distributions. The extracted LE-GMMs features can better distinguish the two types of signals through reasonable and effective mapping. Moreover, the proposed improved deep forest model, MPSForest, not only retains the characteristics of the deep forest learning but also further improves classification accuracy through the multi-pooling and out-of-bag (OOB) error screening mechanisms. And the experiment shows that the multi-pooling method has higher

classification results compared with other pooling methods. This method is evaluated on two intracranial EEG datasets and achieves good classification accuracy superior to several previous methods for the same dataset, which indicates its potential application value for real-time clinical application. Additionally, this technique might be adapted for use in other contexts, such as the brain-machine interface based on EEG signals and the detection of abnormalities in EEG signals.

REFERENCES

[1] A. Anuradha, R. Sara Saji, M.G. Varghese, S. Muthu, and J. C. Prasana, "Vibrational spectroscopic, DFT studies and molecular docking on (2R)-2-acetamido-N-benzyl-3-methoxy propanamide as an antineuropathic pain drug," *Mater. Today: Proc.*, vol. 50, pp. 2615–2622, 2022.

[2] A. Biasiucci, B. Franceschiello, and M.M. Murray, "Electroencephalography," *Curr. Biol.*, vol. 29, no. 3, pp. R80–R85, 2019.

[3] K. Polat and S. Güneş, "Classification of epileptiform EEG using a hybrid system based on decision tree classifier and fast Fourier transform," *Appl. Math. Comput.*, vol. 187, no. 2, pp. 1017–1026, 2007.

[4] Y. Li, Y. Liu, W. G. Cui, Y.-Z. Guo, H. Huang, and Z.-Y. Hu, "Epileptic seizure detection in EEG signals using a unified temporal-spectral squeeze-and-excitation network," *IEEE Trans. Neural Syst. Rehabil. Eng.*, vol. 28, no. 4, pp. 782–794, Apr. 2020.

[5] Y. Ru, J. Li, H. Chen, and J. Li, "Epilepsy detection based on variational mode decomposition and improved sample entropy," *Comput. Intell. Neurosci.*, vol. 2022, pp. 1–11, Jan. 2022.

[6] G. Jaffino, J.P. Jose, and K.S. Kumar, "Expectation-maximization extreme machine learning classifier for epileptic seizure detection," in *Proc. Int. Conf. Forensics Analytics Big Data Secur.*, 2021, pp. 1–5.

[7] D. Epmoghaddam, S. A. Sheth, Z. Haneef, J. Gavvala, and B. Aazhang, "Epileptic seizure prediction using spectral width of the covariance matrix," *J. Neural Eng.*, vol. 19, no. 2, 2022, Art. no. 026029.

[8] Z. Wei, J. Zou, J. Zhang, and J. Xu, "Automatic epileptic EEG detection using convolutional neural network with improvements in time-domain," *Biomed. Signal Process. Control*, vol. 53, 2019, Art. no. 101551.

[9] J. Cao et al., "Unsupervised eye blink artifact detection from EEG with Gaussian mixture model," *IEEE J. Biomed. Health Inform.*, vol. 25, no. 8, pp. 2895–2905, Aug. 2021.

[10] L.M. Patnaik and O. K. Manyam, "Epileptic EEG detection using neural networks and post-classification," *Comput. Methods Programs Biomed.*, vol. 91, no. 2, pp. 100–109, 2008.

[11] W. Hu, J. Cao, X. Lai, and J. Liu, "Mean amplitude spectrum based epileptic state classification for seizure prediction using convolutional neural networks," *J. Ambient Intell. Humanized Comput.*, pp. 1–11, 2019.

[12] Z.H. Zhou and J. Feng, "Deep forest," *Nat. Sci. Rev.*, vol. 6, no. 1, pp. 74–86, 2019.

[13] M. Pang, K.M. Ting, P. Zhao, and Z.-H. Zhou, "Improving deep forest by confidence screening," in *Proc. IEEE Int. Conf. Data Mining (ICDM)*, 2018, pp. 1194–1199.

[14] J. Cheng et al., "Emotion recognition from multi-channel EEG via deep forest," *IEEE J. Biomed. Health Inform.*, vol. 25, no. 2, pp. 453–464, Feb. 2021.

[15] M. Zhou, X. Zeng, and A. Chen, "Deep forest hashing for image retrieval," *Pattern Recognit.*, vol. 95, pp. 114–127, 2019.

[16] W. Liu et al., "Identification of miRNA–disease associations via deep forest ensemble learning based on autoencoder," *Brief. Bioinf.*, vol. 23, no. 3, 2022, Art. no. bbac104.

[17] Y. Guo, S. Liu, Z. Li, and X. Shang, "BCDForest: A boosting cascade deep forest model towards the classification of cancer subtypes based on gene expression data," *BMC Bioinf.*, vol. 19, no. 5, 2018, Art. no. 118.

[18] L.V. Utkin and M.A. Ryabinin, "A siamese deep forest," *Knowl.-Based Syst.*, vol. 139, pp. 13–22, 2018.

[19] A. Shoeibi et al., "Detection of epileptic seizures on EEG signals using ANFIS classifier, autoencoders and fuzzy entropies," *Biomed. Signal Process. Control*, vol. 73, 2022, Art. no. 103417.

[20] M. Baykara and A. Abdulrahman, "Seizure detection based adaptive feature extraction by applying extreme learning machines," *Traitement du Signal*, vol. 38, no. 2, pp. 331–340, 2021.

[21] A. Temko, A. Sarkar, and G. Lightbody, "Detection of seizures in intracranial EEG: UPenn and Mayo Clinic's seizure detection challenge," in *Proc. 37th Annu. Int. Conf. IEEE Eng. Med. Biol. Soc. (EMBC)*, 2015, pp. 6582–6585.

[22] S. Zhang et al., "A combination of statistical parameters for epileptic seizure detection and classification using VMD and NLTWSVM," *Biocybernetics Biomed. Eng.*, vol. 42, no. 1, pp. 258–272, 2022.

[23] Y. Li, W. Cui, M. Luo, K. Li, and L. Wang, "Epileptic seizure detection based on time-frequency images of EEG signals using Gaussian mixture model and gray level co-occurrence matrix features," *Int. J. Neural Syst.*, vol. 28, no. 07, 2018, Art. no. 1850003.

[24] V. Gupta, M. D. Chopda, and R. B. Pachori, "Cross-subject emotion recognition using flexible analytic wavelet transform from EEG signals," *IEEE Sensors J.*, vol. 19, no. 6, pp. 2266–2274, Mar. 2019.

[25] V. Arsigny, P. Fillard, X. Pennec, and N. Ayache, "Fast and simple calculus on tensors in the log-Euclidean framework," in *Proc. Int. Conf. Med. Image Comput. Comput.-Assist. Intervention*, 2005, pp. 115–122.

[26] M. Momeny et al., "Greedy Autoaugment for classification of mycobacterium tuberculosis image via generalized deep CNN using mixed pooling based on minimum square rough entropy," *Comput. Biol. Med.*, vol. 141, 2022, Art. no. 105175.

[27] A. M. Roy, "An efficient multi-scale CNN model with intrinsic feature integration for motor imagery EEG subject classification in brain-machine interfaces," *Biomed. Signal Process. Control*, vol. 74, 2022, Art. no. 103496.

[28] K. Singh and J. Malhotra, "Two-layer LSTM network-based prediction of epileptic seizures using EEG spectral features," *Complex Intell. Syst.*, vol. 8, pp. 1–14, 2022.

[29] L. Zhu, B. Wang, Y. Yan, S. Guo, and G. Tian, "A novel traffic accident detection method with comprehensive traffic flow features extraction," in *Proc. Signal Image and Video Process.*, 2022, pp. 1–9.

[30] G. Keković and S. Sekulić, "Detection of change points in time series with moving average filters and wavelet transform: Application to EEG signals," *Neurophysiology*, vol. 51, no. 1, pp. 2–8, 2019.

[31] K.T. Tapani, S. Vanhatalo, and N. J. Stevenson, "Time-varying EEG correlations improve automated neonatal seizure detection," *Int. J. Neural Syst.*, vol. 29, no. 04, 2019, Art. no. 1850030.

[32] P. Li and Q. Wang, "Local log-euclidean covariance matrix (L^2ECM) for image representation its applications," in *Proc. Eur. Conf. Comput. Vis.*, 2012, pp. 469–482.

[33] M. Zhou et al., "Epileptic seizure detection based on EEG signals and CNN," *Front. Neuroinform.*, vol. 12, 2018, Art. no. 95.

[34] N. Mahmoodian, A. Boese, M. Friebe, and J. Haddadnia, "Epileptic seizure detection using cross-bispectrum of electroencephalogram signal," *Seizure*, vol. 66, pp. 4–11, 2019.

[35] K. D. Tzimourta et al., "A robust methodology for classification of epileptic seizures in EEG signals," *Health Technol.*, vol. 9, no. 2, pp. 135–142, 2019.

[36] G. Liu, W. Zhou, and M. Geng, "Automatic seizure detection based on S-transform and deep convolutional neural network," *Int. J. Neural Syst.*, vol. 30, no. 04, 2020, Art. no. 1950024.

[37] Y. Li et al., "Automatic seizure detection using fully convolutional nested LSTM," *Int. J. Neural Syst.*, vol. 30, no. 04, 2020, Art. no. 2050019.

[38] A. Abugabah, A.A. Alzubi, M. Al-Maitah, and A. Alarifi, "Brain epilepsy seizure detection using bio-inspired krill herd and artificial alga optimized neural network approaches," *J. Ambient Intell. Humanized Comput.*, vol. 12, no. 3, pp. 3317–3328, 2021.

[39] W. Hussain, M.T. Sadiq, S. Siuly, and A. U. Rehman, "Epileptic seizure detection using 1 D-convolutional long short-term memory neural networks," *Appl. Acoust.*, vol. 177, 2021, Art. no. 107941.

[40] J. Mu et al., "Automatic detection for epileptic seizure using graph-regularized nonnegative matrix factorization and Bayesian linear discriminate analysis," *Biocybernetics Biomed. Eng.*, vol. 41, no. 4, pp. 1258–1271, 2021.

[41] S. Yuan et al., "Automatic epileptic seizure detection using graph-regularized non-negative matrix factorization and kernel-based robust probabilistic collaborative representation," *IEEE Trans. Neural Syst. Rehabil. Eng.*, vol. 30, pp. 2641–2650, 2022.

[42] I. Yildiz, R. Garner, M. Lai, and D. Duncan, "Unsupervised seizure identification on EEG," *Comput. Methods Programs Biomed.*, vol. 215, 2022, Art. no. 106604.

[43] J. Zhao et al., "Multilayer weighted integrated self-learning algorithm for automatic diagnosis of epileptic electroencephalogram signals," *Comput. Intell.*, vol. 38, no. 1, pp. 3–19, 2022.